Article ID: 1007-4627(2013) 04-0471-06

Thermal Evolution of Defects in Crystalline Silicon by Sequential Implantation of B and H Ions

ZHANG Bei[1], ZHANG Peng[2], WANG Jun[1], ZHU Fei[1],
CAO Xingzhong[2], WANG Baoyi[2], LIU Changlong[1, 3]

(*1. School of Science, Tianjin University, Tianjin 300072, China;*
2. Key Laboratory of Nuclear Analysis Techniques, Institute of High Energy Physics, Chinese Academy of Sciences, Beijing 100049, China;
3. Tianjin Key Laboratory of Low Dimensional Materials Physics and Preparing Technology, Institute of Advanced Materials Physics Faculty of Science, Tianjin 300072, China)

Abstract: Cz n-type Si (100) wafers were singly or sequentially implanted at room temperature with 130 keV B ions at a fluence of 5×10^{14} cm^{-2} and 55 keV H ions at a fluence of 1×10^{16} cm^{-2}. The implantation-induced defects were investigated in detail by using cross-sectional transmission electron microscopy (XTEM) and slow positron annihilation technique (SPAT). XTEM results clearly show that sequential implantation of B and H ions into Si could eliminate the (111) platelets and promote growth of (100) platelets during annealing. SPAT measurements demonstrate that in B and H sequentially implanted and annealed Si, more vacancy-type defects could remain in sample region around the range of B ions. These results indicate that the promotion effect should be attributed to the role of both B and B implanted induced vacancy-type defects.

Key words: crystalline Si; B and/or H ion implantation; H platelets; XTEM; SPAT

CLC number: O483 **Document code:** A **DOI:** 10.11804/NuclPhysRev.30.04.471

1 Introduction

'Smart-Cut' is a novel, promising production technology of silicon-on-insulator (SOI) systems. Ever since it reported for the first time by Bruel[1], this technology has attracted more attentions and found practical applications in the field of SOI. The 'Smart-Cut' is mainly based on hydrogen implantation and wafer bonding. The standard 'Smart-Cut' technique is confronted by either the high doses or high thermal budget for layer cleavage, which inevitably leads to high cost of production. In order to promote commercial application of such technique, many methods have been presented to reduce the total fluence and annealing temperature for exfoliation[2−4]. Of these methods, sequential implantation of B and H ions has been proved to be effective. For example, Tong et al. demonstrated that a high-quality SOI structure was fabricated at a total fluence of 2.85×10^{16} cm^{-2} [3]. As to the underlying mechanism, some viewpoints have been proposed. Tong et al.[5] considered that a high number of point defects were generated by pre-implanted B ions, and B ions themselves could trap hydrogen atoms. Both processes are likely to assist platelet nucleation and microcrack growth. Höchbauer et al.[6] thought that the presence of non-activated B changed H^+ into H^0/H^-, which is preferable to the formation of H-related platelets. Moreover, Lee et al.[7] demonstrated sequentially implantation of B and H ions into Si could decrease concentration of Si-H defects, which in turn, enhanced H diffusion and the kinetics of blistering.

As a nondestructive method without special sample

Received date: 23 Dec. 2012; **Revised date:** 23 Jan. 2013
Foundation item: National Natural Science Foundation of China (10975107)
Biography: ZHANG Bei(1987–), female, Xingtai, Hebei, China, Master, working on the field of interaction between particles and solids; E-mail: zhangbei@tju.edu.cn.
Corresponding author: LIU Changlong, E-mail: liuchanglong@tju.edu.cn

preparation, slow positron annihilation technique (SPAT) offers an effective way to probe the vacancy-type defects and their evolution in the ion-implanted samples. In the past decades, SPAT has been successfully employed to investigate the Si wafers singly- or sequentially implanted with various kinds of ions, and provided insights in the depth profile of vacancy-type defects together with the complex interplays of defects and implants[8−13]. Nevertheless, to our best knowledge, no relevant study on B and H sequentially implanted Si has been made by using SPAT as yet.

In the present work, we present main results on defects creation in Si singly and sequentially implanted with B and H ions at relatively low fluences. In B and H sequentially implanted Si, promotion effect on thermal growth of (100) H platelets in Si has been well revealed. Moreover, results from SPAT measurements demonstrate that more vacancy-type defects could survive from thermal recombination, which is responsible for the observed promotion effect.

2 Experimental

Cz n-type Si (100) wafers (resistivity of $3 \sim 6\ \Omega\cdot$cm) were used as samples. In this study, three sets of samples were prepared, i.e. samples singly implanted with B ions (labeled as the B sample), samples singly implanted with H ions (the H sample) and samples sequential implanted with B and H ions (the B+H sample), respectively. The B ion implantation was performed at 130 keV with a fluence of 5×10^{14} cm^{-2}, while the H ions were implanted at 55 keV to a fluence of 1×10^{16} cm^{-2}. According to the SRIM 2010 simulations[14], the projected range, R_p, of H ions is a bit larger than that of B ions. Nevertheless, the B profile is nearly overlapped with H implant created vacancy profile, as shown in Fig. 1. After implantation, the samples were furnace annealed in a temperature range from 200 °C to 500 °C for 1 h with a flow of nitrogen gas. Cross-sectional transmission electron microscopy (X-TEM) was selectively used to investigate defect microstructures. Before XTEM observations, the samples were cut, glued, and then thinned using mechanical polishing and ion milling. XTEM images were taken at 200 kV with a JEOL 2010 microscopy. The SPAT was used to characterize the vacancy-type defect profile. During SPAT measurements, slow positrons were implanted with energies tunable between 180 eV and 20 keV. The Doppler broadening of the 511 keV annihilation γ rays was recorded at room temperature. The level of the Doppler broadening is indicated by the parameter S, which is defined as the ratio of the counts in a fixed central region ($|511 - E_\gamma| < 0.85$ keV) of the 511 keV line to the total counts of the peak ($|511 - E_\gamma| < 4.25$ keV). The value of S was normalized to that for virgin Si. The relationship between S and the positron energy E, was analyzed by VEPFIT code, a computer program developed by van Veen et al.[15].

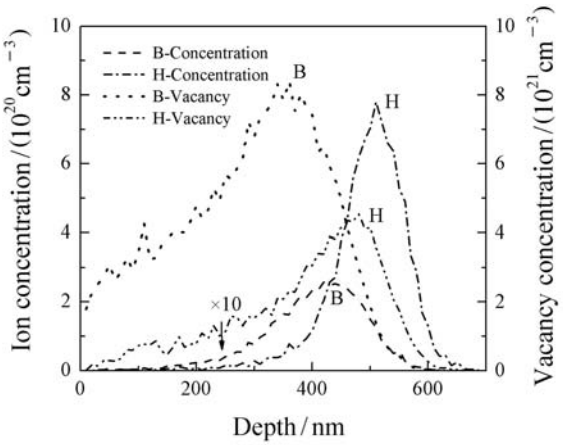

Fig. 1 SRIM simulation results showing depth profiles of B ions, H ions as well as B and H implant induced vacancies in Si under implantation of 130 keV B ions at a fluence of 5×10^{14} cm^{-2} and 55 keV H ions at a fluence of 1×10^{16} cm^{-2}.

3 Results and discussion

Fig. 2 gives the XTEM results of defect microstructures in Si for the H and B+H samples after 500 °C annealing. As shown in Fig. 2(a), 55 keV H ion implantation together with 500 °C annealing creates a well defined damage band into Si. The damage band is centered at about 530 nm with a width of about 80 nm. With a close view of the band (see Fig. 2(b)), one can see that it is mainly made up of (100) platelets, (111) platelets and dislocation loops. The average size of platelets is estimated to be about 20 nm. As to the B+H sample, subsequent 500 °C also produces a well defined damage band (see Fig. 2(c)), which is centered at a nearly same depth as that of the H sample after annealing at the same temperature. However, comparing with the H sample ($\sim$ 80 nm), the band width is evidently large ($\sim$ 125 nm). Fig. 2(d) reveals that the damage band consists of both platelets and dislocations. However,

in such a case, the platelets are mainly lying on (100) habit planes parallel to the sample surface. Moreover, the sizes of platelets significantly increase (30 ∼ 50 nm), accompanying with reduction in their density. The above results clearly show that pre-implantation of B ions could eliminate (111) platelets and promote growth of (100) platelets

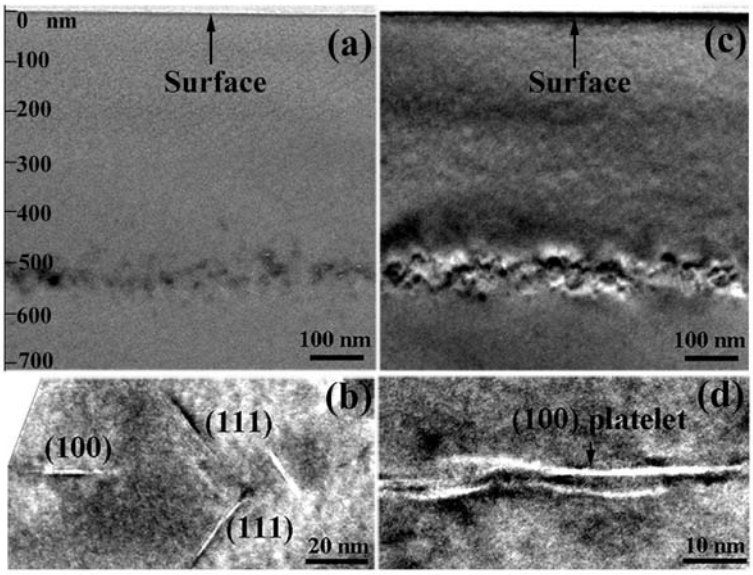

Fig. 2　XTEM micrographs of (a) the H sample and (c) the B+H sample after annealing at 500 °C for 1 hour. (b) and (d) are close views of damage bands in (a) and (c), respectively.

during subsequent annealing.

Fig. 3 shows S parameter versus energy and mean penetration depth of positrons for the B+H sample before and after annealing at different temperatures. The mean penetration depth of positrons into Si, $\bar{z}(nm)$, is approximately calculated by using the expression of $\bar{z} = (A/\rho)E^n$. In the expression, A is a constant of ∼40 for Si, ρ(g/cm^3) is the mass density of the sample, and the index n is chosen to be 1.6 as in the literature[16]. It is clear that the maximum S value in the as-implanted sample occurs around 170 nm, which is about one third of the H projected range according to SRIM simulation. The normalized value is estimated to be about 1.04, indicating that the produced defects are mainly divacancies. However, one can see that the S value is significantly low for sample region around the range of H ions. The low S value in such region could be attributed to role of H in the evolution of defects. Actually, pre-implantation of B ions could generate both vacancy- and interstitial-type defects. During subsequent H implantation, on the one hand, the pre-existing vacancies can easily trap H and form vacancy-hydrogen complex. On the other hand, H atoms could also interact with interstitial dangling bonds, resulting in formation of the Si—H bonds. Moreover, it has been shown that B has the ability to getter

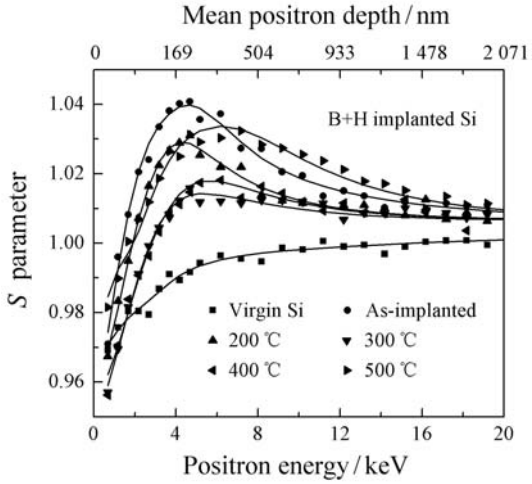

Fig. 3　S parameter vs energy E and mean penetration depth of positrons for the B+H sample before and after annealing at different temperatures. The corresponding curve for the virgin Si is also shown in the same figure for comparison. The lines are best fits to the positron diffusion equation by VEPFIT.

H [17], and thus to form B—H bonds, which causes increase of H concentration around the range of B ions. Therefore, more vacancy-type defects could be passivated by H atoms. After subsequent annealing at temperatures of 200 and 300 °C, reduction in the S parameter is found. Besides disso-

lution of simple vacancy-type defects, reduction of the *S* parameter may also be due to the following two facts. One is that thermal treatment causes decomposition of B—H bonds at 160 °C and above[18], and consequently produces H^+ via the process of $(BH)^0 \rightarrow B^- + H^+$ [19]. Owing to its high diffusion coefficient in Si[20], H^+, which is already locally packed near a B atom, can easily diffuse into nearby vacancy-type defects to form hydrogen molecules. The other is that breakage of Si—H bonds could appear at about 250 °C[21], and more H could take part in evolution of vacancy-type defects. These two processes result in formation of more passivated vacancy-type defects, and thus lead to the decrease in the *S* value. As annealing temperature increases to 400 °C, the *S* value is found to increase accompanied with shift of its peak position to the higher energy, i.e., the deeper position. Actually, H begins to release from the vacancy-hydrogen complexes at temperatures of 400 °C and above[22]. Therefore, vacancy clusters without H can be viewed by penetrating positrons. As the sample was annealed at 500 °C, the *S* parameter continues to increase, suggesting that more and more H or H_2 have been released, and large vacancy clusters free of H are formed by Ostwald Ripening mechanism[23−24]. Finally, a broad and intense *S* peak is detected at a depth corresponding to range of B ions after 500 °C annealing. Moreover, it can be seen that the *S* parameter at high energies (> 10 keV) is still higher than that of the virgin Si, which may be attributed to formation of B clusters owing to migration of B in Si[25].

For the purpose of comparison, SPAT results for the B, H and B+H samples in the as-implanted state and after 500 °C annealing (see Fig. 4) were also presented. From Fig. 4(a), one can see that the *S* values for the B and B+H samples are much higher than that for the H sample. For the B sample, the *S*-*E* curve exhibits a peak around the positron energy of about 6.48 keV, i.e. around a depth of about 340 nm, which coincides with the peak of the vacancy profile induced by B ion implantation. As known from SRIM simulations[14], each implanted B ion (130 keV) can generate $\sim$ 500 vacancies and silicon interstitials, while each H ion (55 keV) can only generate $\sim$10 vacancies. Since *S* parameter reflects the vacancy-type defect concentration, creation of much more vacancy-type defects in the B and B+H samples could contribute to a relatively large *S* value. For the H sample, the *S* peak presents in the near surface region. In the sample region around the H projected range, it affords a low *S* value owing to the fact that most of vacancy-like defects are passivated by H atoms in the form of Si—H bonds. The low *S* value in H passivated vacancy-like defects has been confirmed by lots of researches[11, 26]. As shown in Fig. 4(b), the *S* value around the H damage region for the B+H sample is still much higher than that for the H sample after 500 °C annealing, indicating that more vacancy-type defects in sample region corresponding to the H damage region could survive in the B+H sample. These can well explain the results in Fig. 2. For H atoms, the free energy of the system in the vacancies or platelets is much lower than that when they stay in interstitial places. Thus H atoms are apt to aggregate into the vacancy-type defects created by B ion implantation during subsequent

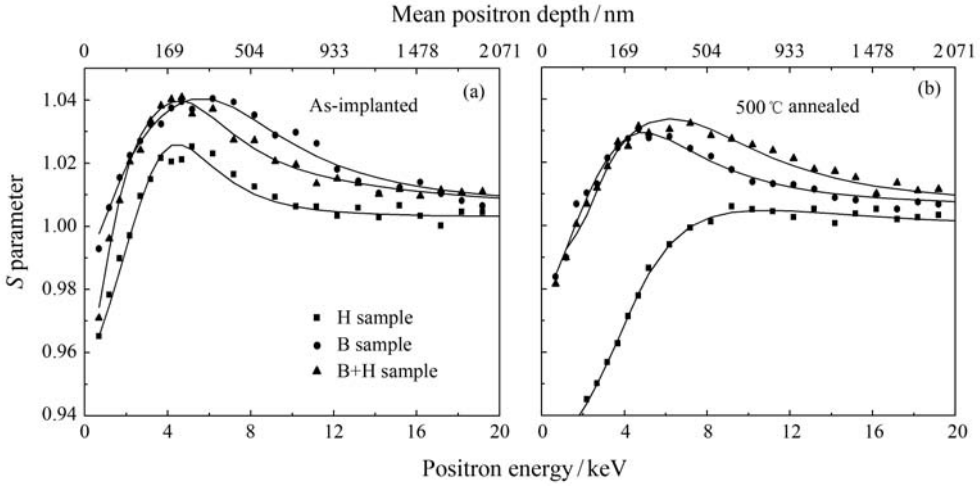

Fig. 4 The *S* parameter vs positron energy *E* for the B sample, H sample and B+H sample (a) before and (b) after 500 °C annealing. The lines are best fits to the positron diffusion equation by VEPFIT.

thermal annealing. Therefore, the dissolution and migration of these defects will be suppressed. Since more and more H atoms accumulate in the vacancies and platelets, in-plane stress and out-of-plane strain could be produced, which result in reduction of the free energy of the plane parallel to the surface. Owing to the fact that our adopted Si sample is (100) oriented, the barrier for H diffusion to the 100 plane decreases. As a result, H platelets with larger sizes could be expected through lateral extension under the inner pressure. Finally the (100) platelets predominantly remain in the B+H sample.

Based on the above results and discussion, the significantly enhanced surface blistering and/or exfoliation observed in the B first and then H implanted Si can be attributed in principle to the interaction between H implants and the B implantation induced vacancies as well as to that between H and B atoms. In the case of H ions followed by B ions, on the one hand, the H implantation formed Si-H complexes can be largely destroyed by the subsequently incident B ions. On the other hand, the H implantation produced Si interstitials may induce the subsequently implanted B atoms to distribute in a wider region via the transient enhanced diffusion (TED) process[27], resultantly leading to a more separated damage zone. Therefore, the surface blistering and/or exfoliation will be suppressed, as demonstrated in the previous works[5, 21, 28]. As for the observed surface blistering and/or exfoliation promotion in the heavily B-doped Si implanted with H ions[5, 29], in our opinion, an enhanced short-distance diffusion of H implants may play a crucial role due to hydrogen trapping by B ions.

4 Conclusions

In conclusion, by using XTEM and SPAT, the defects in B and/or H ion implanted Si have been studied. Pre-implantation of B ions into Si has been found to promote thermal growth of (100) H-platelets, which should be responsible for the enhanced surface exfoliation of B and H co-implanted Si. Based on the SPAT results, we attribute the promotion effect to the role of both B and B implanted induced vacancy-type defects. The finding provides insight on understanding of the mechanism involved in enhanced exfoliation of Si under B and H ion sequentially implantation.

References:

[1] BRUEL M. Electron Lett, 1995, **31**: 1201.

[2] AGARWAL A, HAYNES T E, VENEZIA V C, *et al*. Appl Phys Lett, 1998, **72**: 1086.

[3] TONG Q Y, GOSELE U M. Adv Mater, 1999, **11**: 1409.

[4] MA X B, LIU W L, CHEN C, *et al*. Semicond Sci Technol, 2006, **21**: 959.

[5] TONG Q Y, SCHOLTZ R, GOSELE U, *et al*. Appl Phys Lett, 1998, **72**: 49.

[6] HOCHBAUER T, WALTER K C, SCHWARZ R B, *et al*. J Appl Phys, 1999, **86**: 4176.

[7] LEE J K, HOCHBAUER T, AVERITT R D, *et al*. Appl Phys Lett, 2003, **83**: 3042.

[8] BRUSA R S, KARWASZ G P, TIENGO N, *et al*. J Appl Phys, 1999, **85**: 2390.

[9] EICHLER S, GEBAUER J, BORNER F, *et al*. Phys Rev B, 1997, **56**: 1393.

[10] KRUSEMAN A C, SCHUT H, VAN VEEN A, *et al*. Nucl Instr and Meth B, 1999, **148**: 294.

[11] FUJINAMI M, SUZUKI R, OHDAIRA T, *et al*. Phys Rev B, 1998, **58**: 12559.

[12] DUO X Z, LIU W L, ZHANG M, *et al*. J Appl Phys, 2001, **90**: 3780.

[13] LIU Changlong. Nuclear Physics Review, 2004, **21**(3): 231. (in Chinese)
(刘昌龙. 原子核物理评论, 2004, **21**(3): 231.)

[14] ZIEGLER J F, BIERSACK J P. SRIM (Stopping and Range of Ions in Matter) computer code[EB/OL]. [2012-10-09]. http://www.srim.org.

[15] VAN V A, SCHUT H, de VRIES J, *et al*. AIP Conf Proc, 1990, **218**: 171.

[16] HUANG L J, LAU W M, SIMPSON P J, *et al*. Phys Rev B, 1992, **46**: 4086.

[17] BORENSTEIN J T, CORBETT J W, PEARTON S J. J Appl Phys, 1993, **73**: 2751.

[18] CHANDRASEKHAR M, CHANDRASEKHAR H R, GRIMSDITCH M, *et al*. Phys Rev B, 1980, **22**: 4825.

[19] DENTENEER P J H, van de WALLE C G, PANTELIDES S T. Phys Rev B, 1989, **39**: 10809.

[20] PEARTON S J. Mater Sci Eng B, 1994, **23**: 130.

[21] TERREAULT B. Phys Stat Sol (a), 2007, **204**: 2129.

[22] FUJINAMI M, SUZUKI R, OHDAIRA T, *et al*. Appl Surf Sci, 1999, **149**: 188.

[23] EVANS J H. Nucl Instr and Meth B, 2002, **196**: 125.

[24] LI Bingsheng, ZHANG Chonghong, YANG Yitao, *et al*. Nuclear Physics Review, 2008, **25**(2): 144. (in Chinese)
(李炳生, 张崇宏, 杨义涛, 等. 原子核物理评论, 2008, **25**(2): 144.)

[25] NAPOLITANI E, de SALVADOR D, STORTI R, *et al*. Phys Rev Lett, 2004, **93**: 055901.

[26] UEDONO A, MORI T, MORISAWA K, *et al*. J Appl Phys, 2003, **93**: 3228.
[27] SADIGH B, LENOSKY T J, THEISS S, *et al*. Phys Rev Lett, 1999, **83:** 4341.
[28] NURMELA A, HENTTINEN K, SUNI T, *et al*. Nucl Instr and Meth B, 2004, **219:** 747.
[29] DESROSIERS N, GIGUERE A, MOUTANABBIR O, *et al*. Appl Phys Lett, 2005, **87**: 231908.

B 和 H 离子顺次注入单晶 Si 引起的缺陷及其热演变

张 蓓[1]，张 鹏[2]，王 军[1]，朱 飞[1]，曹兴忠[2]，王宝义[2]，刘昌龙[1, 3]

(1. 天津大学理学院物理系，天津 300072；
2. 中国科学院高能物理研究所核分析技术重点实验室，北京 100049；
3. 天津市低维功能材料物理与制备技术重点实验室，天津 300072)

摘要： 室温下将 130 keV，5×10^{14} cm^{-2} B 离子和 55 keV，1×10^{16} cm^{-2} H 离子单独或顺次注入到单晶Si中，采用横截面试样透射电子显微镜(XTEM)和慢正电子湮没技术 (SPAT) 研究了离子注入引起的微观缺陷的产生及其热演变。XTEM 观测结果显示，B 和 H 离子顺次注入到单晶 Si 可有效减少 (111) 取向的H板层缺陷，并促进了 (100) 取向的 H 板层缺陷的择优生长。SPAT 观测结果显示，在顺次注入的样品中，B 离子平均射程处保留了大量的空位型缺陷。以上结果表明，B 离子本身及 B 离子注入所产生的空位型缺陷对板层缺陷的生长起到了促进作用。

关键词： 单晶 Si；B 和 H 离子注入；H 板层缺陷；XTEM；SPAT

收稿日期： 2012-12-23； **修改日期：** 2013-01-23
基金项目： 国家自然科学基金资助项目(10975107)
通信作者： 刘昌龙, E-mail: liuchanglong@tju.edu.cn